Laser-Cooled Trapped-Ion Experiments at NIST[1]

Joseph N. Tan, J. J. Bollinger, A. S. Barton, and D. J. Wineland

Time and Frequency Div., National Institute of Standards and Technology, 325 Broadway, Boulder, CO 80303

Abstract. We describe some recent experiments that use a new Penning trap to trap and laser-cool more than 10^5 Be^+ ions. In this work the Coulomb coupling parameter was estimated to be typically greater than 100 and in some cases greater than 300. Shell structure was difficult to observe in the ion fluorescence from these large clouds. An initial Bragg scattering experiment to obtain information on the ion correlations is described. We also briefly review our work on the electrostatic modes of a Penning trap plasma, including the use of the modes to diagnose the shape and density of a cryogenic electron plasma. Some applications of laser-cooled plasmas in Penning traps, such as atomic clocks, are discussed.

I. INTRODUCTION

At the National Institute of Standards and Technology (NIST) in Boulder, laser-cooled ions stored in Penning (1) and rf or Paul (1) traps are used for plasma studies, high precision spectroscopy, and atomic clocks. In this manuscript we discuss aspects of our trap work which involve the nonneutral plasma physics of large systems of confined ions. We concentrate on experiments in Penning traps because these studies involve plasmas of a few hundred thousand trapped ions while in our rf trap work, only a few or perhaps a few tens of ions are trapped. Penning traps have been used at NIST to trap electrons (2), Mg^+ (3,4), Be^+ (5-9), and Hg^+ (10) ions. Reference 11 reviews some of this work. Here we discuss some of our recent work on $^9Be^+$ ions (12) and electrons.

Ion confinement in a Penning trap can be extremely long (> 1 day). Therefore the trapped ions have sufficient time to evolve to a state of global thermal equilibrium (13,14,15). (Measurements indicate that our trapped ion plasmas evolve to a spatial distribution consistent with global thermal equilibrium (6). However, in some cases

---

[1]Work of the U. S. Government, not subject to copyright.

motion parallel and perpendicular to the magnetic field may have different temperatures (5,6).) In thermal equilibrium, the rotation (at frequency ω_r) of the ions about the magnetic field axis is uniform or "rigid" (6,14). An important advantage of using ions in plasma studies is that the atomic structure of the ions can be used to manipulate the equilibrium state of the plasma. Doppler laser-cooling (16), for instance, is now routinely used to reach temperatures less than 10 mK for small Be^+ plasmas. The Doppler-cooling limit for Be^+ is 0.5 mK. In addition to cooling the ions, laser beams are used to apply a torque on the ion plasmas and change or control the ion density (8).

Laser-cooling yields ion plasmas in which the Debye length λ_D is much less than the plasma dimensions. In this case the plasma has a uniform density $n_0 = 2\epsilon_0 m\omega_r(\Omega-\omega_r)/q^2$ with a sharp boundary. Here q and m are the charge and mass of the ion, Ω=qB/m is the ion cyclotron frequency, ϵ_0 is the permittivity of the vacuum, and B is the magnetic field of the Penning trap. In our experimental work, the plasma dimensions are very much smaller than the trap dimensions, typically by more than a factor of 10. In this case, the trap potential is quadratic in the region of the ion plasma. We let ω_z denote the harmonic oscillation (or axial bounce) frequency of a single ion in the trap. When λ_D is much less than the plasma dimensions and the plasma dimensions are much less than the trap dimensions, a Penning trap plasma is a uniform density spheroid (an ellipse rotated about one of its symmetry axes) (6,17,18). Let $2z_o$ denote the axial extent of the plasma spheroid at r = 0 and $2r_o$ denote the plasma diameter at $z = 0$. The aspect ratio $\alpha = z_o/r_o$ of the spheroid is determined (6,17) by ω_r, Ω, and ω_z.

The aspect ratio of an ion plasma as a function of ω_r can be understood by examining the radial confining force acting on ions as they rotate through the magnetic field in a Penning trap. Due to the plasma rotation, the ions experience a $\vec{v} \times \vec{B}$ Lorentz force which pushes radially inward. For low rotation frequencies (slightly greater than the single ion magnetron frequency ω_m), this radial confining force is weak resulting in a pancake-shaped or oblate plasmas. As ω_r increases, the radial confining force grows, and the plasma density and aspect ratio increase. The highest density and largest plasma aspect ratio are obtained at the Brillouin limit where $\omega_r = \Omega/2$. For higher rotation frequencies, the centrifugal acceleration, which increases as ω_r^2, overcomes the radial binding force and the plasma once again becomes an oblate spheroid.

II. EXPERIMENTAL APPARATUS

Figure 1 shows a diagram of the electrode structure of the Penning trap we are currently using to trap Be^+ ions. The apparatus, which consists of two separate traps, is enclosed in a room-temperature vacuum jacket (10^{-8} Pa) and centered in the vertical bore of a homogeneous, 4.5 T superconductive magnet. With the use of plasma modes (8,9), the symmetry axis of the electrode assembly is aligned to within

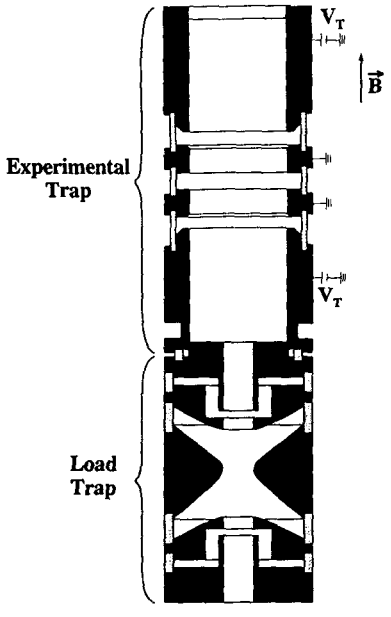

Figure 1. Cross section of the Penning trap used to trap plasmas of Be^+ ions. The dark shaded parts are copper electrodes. The light shaded parts are ceramic insulators. Ions are created in the load trap and then transferred to the experimental trap. The experimental trap electrodes are right circular cylinders with a 2.0 cm diameter inner radius. They provide a quadratic potential near the trap center. Laser beams pass through gaps in the insulators between the electrodes or vertically along the trap axis. Compensation electrodes (not shown) are mounted on the insulators in the experimental trap. In recent work, B=4.5 T and V_T ranges from 10 V to about 1.5 kV. For Be^+ ions this gives a cyclotron frequency of 7.6 MHz and a trap axial frequency ranging from 80 to 980 kHz.

0.01° of the applied magnetic field direction.

The load trap has electrode surfaces machined to lie on hyperboloids of revolution. It is used for producing ions and for ejection of impurity ions. Ions are loaded by ionizing neutral atoms in the trap with a beam of electrons that pass through the endcaps. Small atomic ovens provide the source of neutral atoms. A hyperbolic Penning trap provides a large volume over which the electrostatic potential is quadratic, which improves the resonant ejection of impurity ions using an rf field. The symmetry of the load trap is degraded by the holes and slits required for the atomic ovens and electron guns, and by patch effects due to the atomic beams plating onto the electrodes. Laser cooling and imaging optics (f/7 input) are provided so that crude mass spectrometry can be performed to check for impurity ions.

From the load trap, the collected ions are transferred along the magnetic field direction into a precision cylindrical Penning trap (the experimental trap in Fig. 1). The potentials applied to the electrode assembly are varied slowly to adiabatically shift the axial trapping well from the center of the (hyperbolic) load trap to the center of the (cylindrical) experimental trap. The electrodes of the experimental trap form a 12.7 cm long stack (including gaps) of OFHC copper rings. In each gap between the cylindrical electrodes are compensation electrodes divided into six equal sectors with 0.64 cm separation between neighboring sectors. The compensation electrodes allow rf excitation of plasma modes and minimization of small azimuthal asymmetries. The separation between neighboring compensation electrodes permits optical access to the

trap center. For spectroscopy experiments, a nuclear spin flipping rf drive can be coupled to the ions through one of these gaps. A microwave drive can also be applied for measurements of ω_r from the Doppler shift of an electron spin flip transition (8).

A new feature of this apparatus is the ability to simultaneously image the ions in two orthogonal directions. The optical axis of an f/2 system is aligned with the symmetry axis of the trap and provides a top-view image of the ions. Perpendicular to the magnetic field, an f/5 optical system is used to obtain a side-view image of the ion plasma. This side-view image gives the spheroidal boundary of the plasma. The density and rotation frequency of the plasma can be determined from the aspect ratio of such an image.

III. STRONG COUPLING

In a frame of reference rotating with the ions, ions in a Penning trap behave as if they are immersed in a uniform density background of opposite charge (19), where the trapping fields provide the uniform background of opposite charge. A single species of charge immersed in a uniform density background of opposite charge is a one-component plasma (20). The thermodynamic properties of a one-component plasma are determined by the Coulomb-coupling parameter

$$\Gamma = \frac{q^2}{4\pi\epsilon_o a_S k_B T}, \qquad (1)$$

where a_S is the Wigner-Seitz radius given by $4\pi n_0 a_S^3/3 = 1$ and T is the ion temperature. Calculations (20,21) for the infinite one-component plasma predict that for $\Gamma > 2$, the plasma should exhibit liquid-like behavior characterized by short range order, and at around Γ=170 a liquid-solid phase transition to a body-centered cubic (bcc) lattice should take place. With laser cooling, coupling parameters of several hundred can be routinely obtained with ions in traps (5,13). In principle, with Be^+ ions at the Doppler laser-cooling limit of 0.5 mK and the Brillouin density at B=4.5 T of 5.9×10^9 cm^{-3}, the coupling parameter can be as high as 9700.

A. Shell structure

Ion trap experiments until now have laser-cooled small plasmas. Typical plasma dimensions are less than 20 interparticle spacings (7). (In the quadrupole storage ring trap of Ref. 22, the plasmas were dimensionally large along the quadrupole circumference, but less than 8 interparticle spacings in the other directions.) Such small systems should not behave like infinite-volume one-component plasmas. Computer simulations (23,24,25) with less than a few thousand cold ions in a trap

found something quite different than bcc order. The ions eventually solidified into concentric, approximately spheroidal shells rather than bcc planes.

Experimentally, shell structure has been observed with up to 20 000 laser-cooled Be^+ ions in a Penning trap (7). [Analogous shell structure has also been observed in a miniature rf storage ring trap (22).] The shells were observed by illuminating a thin cross section of the plasma with laser beams and imaging the laser-induced fluorescence onto a photon-counting imaging tube. Imaging works well for observing shell structure because the structure is preserved by the plasma rotation. Qualitative agreement was observed with the simulations (7), except that, in some cases, open-ended cylindrical shells were observed in the experiments. The cause of these open-ended shells remains an open question. One possibility is that shear in the plasma rotation might produce such a structure.

So far the observed ion correlations (shell structure) are strongly affected by the finite size and boundary of the plasma. How large must the ion plasmas be in order to exhibit infinite-volume behavior? Two different analytical methods (26,27) give similar predictions. The plasmas may have to be greater than 60 interparticle spacings along their smallest dimension in order to exhibit bcc structure. A spherical plasma with 60 shells has about 10^6 trapped ions.

B. Bragg scattering

In the trap shown in Fig. 1, we measured the densities and temperatures of plasmas of several hundred thousand laser-cooled Be^+ ions. Only the temperature parallel to the magnetic field was measured. These measurements indicated that the plasmas were strongly coupled with couplings typically greater than 100 and in some cases greater than 300. Shell structure has been difficult to observe in the images of these larger plasmas. In some cases, shells were observed near the plasma boundary, but not in the plasma interior. As the clarity of the shells decreases with increasing ion number, a different technique is required to obtain information on the ion correlations.

Bragg scattering (28) can be used to obtain this information. The Bragg scattering signal as a function of the scattering angle is just the Fourier transform of the ion pair correlation function. The relative positions and heights of the Bragg scattering peaks therefore give information on the spacings and relative positions of the ions in the strongly coupled plasma. For example, in our experimental setup, a laser beam (with frequency tuned slightly below the cooling transition) can be directed along the symmetry axis of the trap with a beam waist large enough to encompass the ion plasma. Light is approximately elastically scattered from the ions and will interfere constructively in certain directions. Because the 313 nm wavelength of our cooling laser is small compared to the inter-ion spacing (from 15 to 5 μm depending on the density), constructive interference will occur mainly in the forward-scattered light. We estimate that the first and strongest Bragg scattering peak will occur at a

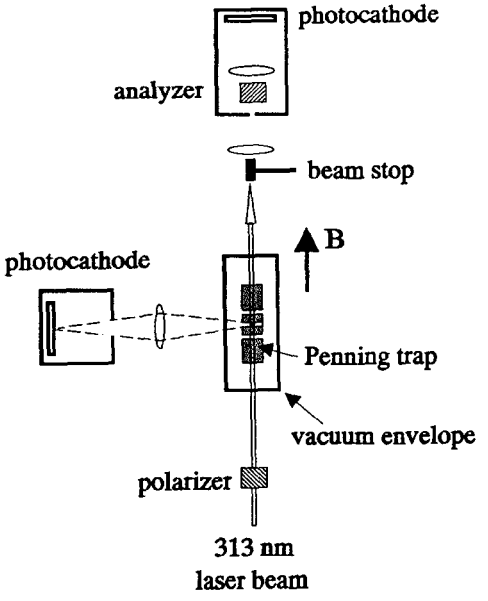

Figure 2. Schematic diagram of the Bragg scattering setup. A 313 nm laser beam is directed through the ions along the magnetic field axis and then blocked by a beam stop. The forward-scattered ion fluorescence is observed as a function of the scattering angle. Light scattered off the laser windows is minimized by an aperture at an image of the ions and with a pair of crossed polarizers (the polarizer and analyzer). An image of the ion plasma is obtained from light scattered at 90° from the magnetic field direction.

small scattering angle between 1 and 3°.

Very recently at NIST, Bragg scattering from Be^+ ions in a Penning trap has been observed. The detection system was designed to separate the forward-scattered ion fluorescesce from the background of forward-scattered light off the vacuum windows. A simple sketch of the experimental set-up is given in Fig. 2. The laser beam is linearly polarized and is blocked by a beam stop after passing through the vacuum chamber. Two steps were taken to minimize the forward-scattered background light. First, because the ion fluorescence is mainly circularly polarized along the direction of observation (close to the $\vec{B}$-field direction) and the forward-scattered light from the windows is mainly linearly polarized, a pair of crossed polarizers can be used to preferentially attenuate the forward-scattered background light. Second, an image of the ion fluorescence was formed in the center of a small aperture. This aperture helped skim off some of the forward-scattered background light. The Bragg scattered light was then observed with a photon-counting camera. With these steps, it was possible to observe Bragg scattering off plasmas of 3×10^4 ions with good signal-to-noise ratio. Figure 3 shows an example of the observed Bragg scattering pattern. The positions of the first two Bragg peaks provide some information on the

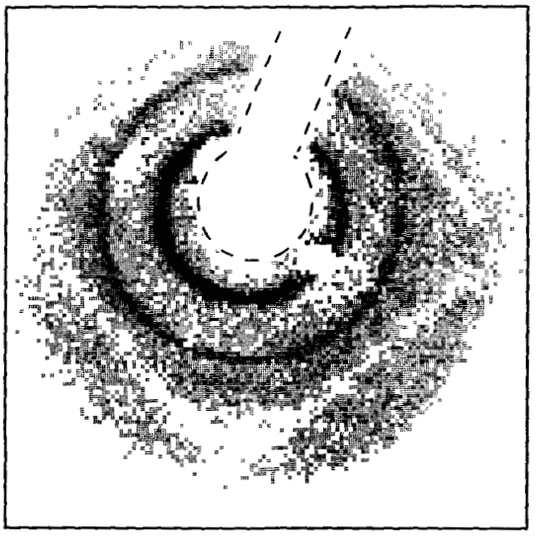

Figure 3. Bragg scattering image observed with approximately 3×10^4 Be^+ ions. The first two Bragg peaks are visible. The ion density here was about 9% of the Brillouin density which produced a scattering angle for the first peak of about 1.5°. The square shadow near the edge of the image is from a wire mesh on the top of the upper experimental trap endcap. The dashed line outlines the beam stop.

type of ion spatial correlations. We are in the process of analyzing this information.

IV. ELECTROSTATIC MODES

A cold nonneutral plasma stored in a Penning trap where the plasma dimensions are small compared to the trap is a constant density spheroid. The electrostatic modes of a spheroidal plasma in a uniform magnetic field can be calculated exactly (29). The modes can be described (9,29) with the use of spheroidal coordinates by two integers (ℓ,m) with $\ell\geq1$ and $m\geq0$. (Negative values of m are allowed but do not give rise to new modes.) The index m indicates that the plasma mode displays an $\exp(im\phi)$ dependence where ϕ is the azimuthal angle. The index ℓ describes the mode dependence along a spheroidal surface (for example, the plasma boundary) in a direction perpendicular to $\hat{\phi}$. As an example, the $\ell=1$ modes are the familiar center of mass modes. Plasma modes have been detected in two different experiments at NIST (2,8,9). In one experiment, some of the $\ell=2$ modes were excited on plasmas of laser-cooled Be^+ ions (8,9). Laser torques were used to vary the plasma rotation frequency. The rotation frequency could be measured from Doppler shifts induced by the rotation. In this way the theoretical predictions for the mode frequencies were tested at the level of a few percent. The new trap shown in Fig. 1 has segmented compensation electrodes which should permit the excitation of azimuthally

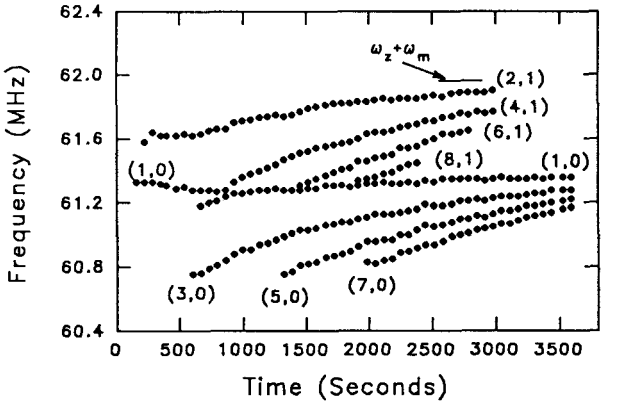

Figure 4. A plot of the measured cryogenic electron plasma mode frequencies vs time after the plasma was loaded into the trap. The modes are labeled by their (ℓ,m) values. The measurement uncertainty in the frequency is less than the symbol size used in the plot and is the same for all points.

asymmetric modes and extend the studies in Refs. 8 and 9. Measurement of the modes can be a useful tool in diagnosing the plasma density and shape. This should be particularly useful for antimatter (30,31,32) and electron plasmas where the standard techniques for obtaining this information involves dumping the plasma out of the trap. Plasma modes have been used as a diagnostic tool in several experiments (2,33,34). At NIST plasma modes have been used to obtain information on the aspect ratio and density of a cryogenic electron plasma (2).

In the NIST experiment the modes were detected by spectrum analyzing the image currents induced in one of the endcap electrodes of a Penning trap at cryogenic (4 K) temperatures. Experimentally, modes with frequencies near the single-particle axial frequency ω_z could be detected. Immediately after a plasma of electrons was loaded into the trap, only the center-of-mass mode was observed. However, after a time that depended on the magnetic field, other modes were observed. The evolution of the mode frequencies was followed as a function of time as shown in Fig. 4. The detected modes were identified within the framework of Dubin's cold fluid theory (29) as drumhead modes of a 2-dimensional disk. In Fig. 4, we identified 8 modes which were used to provide 7 different estimates of the plasma aspect ratio shown in Fig. 5. The discrepancy between the different estimates is on the order of 20 %. Figure 5 shows that the drumhead modes were detected when the plasma aspect ratio α was about 0.02 or smaller. The decrease in α as a function of time could then be followed until $\alpha \approx 0.002$. The number of electrons, determined from the center-of-mass mode signal (35), varied from 20 000 to 100 000. The modes observed here may be related to the features observed in Ref. 36. This experiment also demonstrated compression of the electron plasma by a "sideband cooling drive" at frequency $\omega_z+\omega_m$.

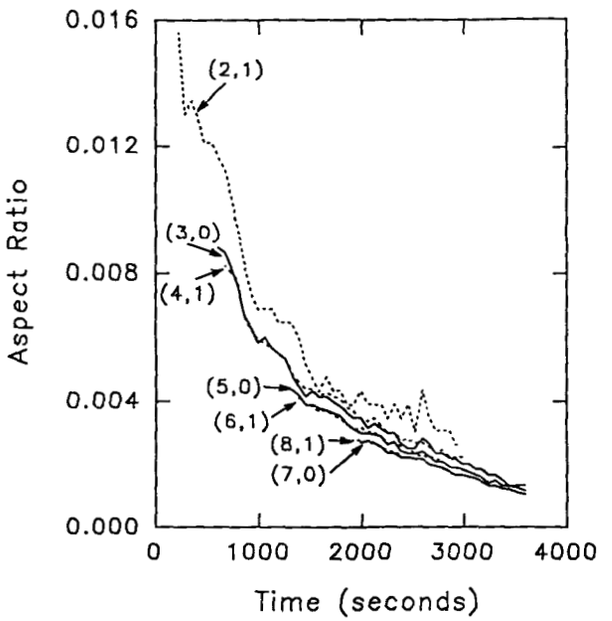

Figure 5. Estimates of the plasma aspect ratio α as a function of the time after the plasma was loaded, for the data of Fig. 4. For each time, the (1,0) mode is used to estimate ω_z. Each (ℓ, m) mode (except the (1,0) mode) is then used to estimate α as described in Ref. 2. The estimated values of α have been connected by straight lines for each mode. The values of α from m=1 (m=0) modes are connected by dashed (solid) lines.

V. APPLICATIONS OF PENNING TRAP PLASMAS

A. Spectroscopy

Ion traps have several properties which are useful for high-resolution spectroscopy. The fact that the ions are stored means their velocity averages to 0; this virtually eliminates the first order Doppler shift of ion spectra. Long storage times can lead to very high resolution; linewidths smaller than 0.001 Hz have been observed (37). Ions are typically stored under high vacuum conditions; this minimizes perturbations of the ions' internal structure caused by background gas collisions. The Coulomb repulsion between ions has both bad and good effects. It limits the attainable density and therefore the overall numbers of ions; this limits the signal-to-noise ratio, thereby limiting the measurement precision (38). On the other hand, the Coulomb repulsion reduces the perturbing effects of ion-ion collisions; this is particularly true at low temperatures where the ions never get very close together.

One application of high-resolution spectroscopy is the determination of atomic structure and measurement of nuclear moments. Another application is atomic clocks and frequency standards. Atomic clocks generate time intervals by counting the cycles of an oscillator which is made synchronous with the natural oscillations in atoms. The first frequency standard using a Penning trap and the first using laser-cooled atoms was demonstrated with a hyperfine transition in $^9Be^+$ ions (39). It had an accuracy of about 1 part in 10^{13} limited in part by an (unexpected) large pressure shift due to background gas molecules (40). (At present, the most accurate atomic clocks have inaccuracies of about 1 part in 10^{14}.) This shift could reduced by many orders of magnitude by cryogenic cooling.

We anticipate that the largest systematic frequency shift in a clock based on stored ions in a Penning trap will be the time-dilation shift caused by the rotational speed of the ions in the plasma (41). (We assume that the cyclotron and axial temperatures are reduced to low enough values that the contribution to the overall speed of the ions due to these components of the motion is negligible.) Recently we investigated this problem theoretically and found that the time-dilation shift due to the velocity of rotation of the ions can be minimized by preparing the ions in a special spheroid (42). For very low ($\omega_r \rightarrow \omega_m$) and very high ($\omega_r \rightarrow \Omega - \omega_m$) rotation frequencies, the spheroid is stretched into a thin circular disk ($\alpha \rightarrow 0$ if the $\vec{v} \times \vec{B}$ radial restoring force is weak or the centrifugal force is large), and consequently, the time-dilation shift for the thin disk of ions is very large. The time dilation shift goes to a minimum at a particular (low) value of ω_r which brings the ions closer to the trap axis. Near this minimum there is only a second-order dependence on rotation frequency, and thus greater frequency stability can be obtained. This is illustrated in Table 1.

Table 1. Expected performance for Penning-trap-based frequency standards which use hyperfine transitions. We assume 10^6 ions, $r_o = 4.2$ mm, and $z_o/r_o = 0.46$. The fractional measurement uncertainty ($\sigma_y(\tau) = \delta\nu(\text{measurement})/\nu_o$) is evaluated as described in Ref. 41. The fractional time dilation shift is $\Delta\nu/\nu_o$. If the fluctuations in plasma radius are held to 5% of the optimal radius, the fluctuations in $\Delta\nu/\nu_o$ are 1% of the last column. (From Ref. 42)

Ion	ν_0 (GHz)	B (T)	$\sigma_y(1\text{ s}) \times 10^{15}$	minimum $\Delta\nu/\nu_o \times 10^{15}$
$^9Be^+$	0.303016	0.8194	53	-241
$^{25}Mg^+$	0.291996	1.2398	55	-105
$^{67}Zn^+$	≈1	≈8.0	16	-2.5
$^{199}Hg^+$	20.9	43.9	0.76	-0.84
$^{201}Hg^+$	7.73	3.91	2.1	-11

B. Multiple species plasmas

Two or more ion species (of the same sign of charge) can be stored simultaneously in a Penning trap in thermal equilibrium. At low enough temperatures, the species separate spatially due to differences in centrifugal forces; the ions with the highest charge-to-mass ratio are pushed to the center of the ion cloud and form a column on the axis (43). For densities sufficiently below the Brillouin density, the separation between the ion species can be approximately equal to the mean interparticle spacing so the thermal contact between ions can remain fairly strong. This can be useful in different kinds of experiments. For example, if one of the stored species is an ion which can be laser cooled, this cooling can be transferred to the second species - "sympathetic" laser cooling (10). This technique was useful in the $^9Be^+$ Penning trap clock experiments. There, laser cooling could not be applied directly to the $^9Be^+$ ions when the clock transition was being driven (durations ≈ 100 s) because of the large "light" shifts of the clock levels caused by the laser. On the other hand, if cooling had not been provided continuously, the ions would have heated leading to a relatively large time-dilation shift (39). Therefore, simultaneously stored laser-cooled Mg^+ ions were used to keep the $^9Be^+$ ions cold (48).

Sympathetic laser cooling may also be useful to cool ion species where no other direct means of cooling is available. If the cooling laser is also used to compress the laser-cooled species through laser-induced torque, this torque is also sympathetically transferred to the other species thereby preventing or reversing radial diffusion. The transfer of cooling and torque may be useful, for example, in experiments which capture high-Z ions from other sources such as storage rings or electron beam ion sources (44). At NIST we have recently become interested in experiments which capture and cool positrons in a Penning trap through collisions with a laser-cooled $^9Be^+$ ion plasma. We have analyzed this problem theoretically by making estimates of capture efficiencies under possible experimental conditions (45). (We have refined the basic idea outlined in Ref. 45 and are preparing a manuscript on this). The idea is as follows: positrons from a moderated ^{22}Na source are assumed to be captured in the trap through Coulomb collisions with the $^9Be^+$ ions. Once the positrons are trapped, cooling will occur through sympathetic cooling with the $^9Be^+$ plasma and positron cyclotron radiation. As the positrons cool, a centrifugal separation will occur between the positrons and the $^9Be^+$ ions and force the positrons to coalesce into a cold column along the trap axis. We have analyzed an experiment for a cylindrical Penning trap with B = 6 T. In this field, a laser-cooled $^9Be^+$ plasma can reach a uniform density of up to 10^{10} cm^{-3} based on our previous studies (8). Positrons from a ^{22}Na source will enter the UHV trap region axially through a thin Ti foil. After passing through the plasma, the positrons will strike a Cu(111) single crystal moderator and about 0.1 % will emerge backwards towards the trap as a beam of slow positrons. Some of these positrons will lose enough axial energy through Coulomb collisions with the $^9Be^+$ plasma to remain trapped. A Monte-Carlo simulation indicates a capture efficiency of greater than 10% of the moderated positrons for a $^9Be^+$ density of 10^{10}

atoms/cm^3 and a column length of about 1 cm. Given a 2 mCi positron source, we expect to capture positrons at a rate of 2800 s^{-1} for these conditions. The resulting dense reservoirs of cold positrons may be useful for antihydrogen production (46) and for reaching a plasma state in which the mode dynamics must be treated quantum mechanically.

C. Other studies

Many other uses of Penning traps are described in papers from this workshop (see also Ref. 44). At NIST we have used the high measurement precisions and accuracies obtained from spectra on ions in Penning traps to perform accurate tests of physical laws. For example, Penning traps have been used to make precise tests of Local-Lorentz invariance (47) and the linearity of quantum mechanics (48), and they have allowed searches for anomalous spin interactions (49). We have also used the high detection sensitivity capable of detecting transitions in individual atoms to study various quantum effects in measurements such as "quantum jumps" (50), the "quantum Zeno" effect (51), and quantum "projection" noise (38). Starting with the early Penning trap experiments at NIST (3), we have also performed many experiments and theoretical studies on laser cooling in Penning traps. The NIST work has been summarized in several Technical Notes (52) (available upon request).

ACKNOWLEDGEMENTS

We gratefully acknowledge the support of the U. S. Office of Naval Research. We thank Brana Jelenkovic, John Miller, and Matt Young for their suggestions and careful reading of the manuscript.

REFERENCES

1. H.G. Dehmelt, Adv. At. Mol. Phys. **3**, 53 (1967); **5**, 109 (1969); D.J. Wineland, W.M. Itano, and R.S. Van Dyck, Jr., ibid **19**, 135 (1983); R.C. Thompson, Adv. At. Mol. Opt. Phys. **31**, 63 (1993).
2. C.S. Weimer, J.J. Bollinger, F.L. Moore, and D.J. Wineland, Phys. Rev. A **49**, 3842 (1994).
3. D.J. Wineland, R.E. Drullinger, and F.L. Walls, Phys. Rev. Lett. **40**, 1639 (1978).
4. W.M. Itano and D.J. Wineland, Phys. Rev. A **24**, 1364 (1981).
5. J.J. Bollinger and D.J. Wineland, Phys. Rev. Lett. **53**, 348 (1984).
6. L.R. Brewer, J.D. Prestage, J.J. Bollinger, W.M. Itano, D.J. Larson, and D.J. Wineland, Phys. Rev. A **38**, 859 (1988).
7. S.L. Gilbert, J.J. Bollinger, and D.J. Wineland, Phys. Rev. Lett. **60**, 2022 (1988).
8. D.J. Heinzen, J.J. Bollinger, F.L. Moore, W.M. Itano, and D.J. Wineland, Phys. Rev. Lett. **66**, 2080 (1991).
9. J.J. Bollinger, D.J. Heinzen, F.L. Moore, W.M. Itano, and D.J. Wineland., Phys. Rev. A **48**, 525

(1993).
10. D.J. Larson, J.C. Bergquist, J.J. Bollinger, W.M. Itano, and D.J. Wineland, Phys. Rev. Lett. **57**, 70 (1986).
11. J.J. Bollinger, D.J. Wineland, and D.H.E. Dubin, Phys. Plasmas **1**, 1403 (1994).
12. J.N. Tan, J.J. Bollinger, and D.J. Wineland, Bull. Am. Phys. Soc. **38**, 1972 (1993).
13. R.C. Davidson, "Physics of Non-Neutral Plasmas" (Addison-Wesley, Redwood City, CA, 1990).
14. C.F. Driscoll, J.H. Malmberg, and K.S. Fine, Phys. Rev. Lett. **60**, 1290 (1988).
15. S.A. Prasad and T.M. O'Neil, Phys. Fluids **22**, 278 (1979).
16. D.J. Wineland and W.M. Itano, Phys. Today 40(6), 34 (1987).
17 D.J. Wineland, J.J. Bollinger, W.M. Itano, and J.D. Prestage, J. Opt. Soc. Am. B**2**, 1721 (1985).
18. J.B. Jeffries, S.E. Barlow, and G.H. Dunn, Int. J. Mass Spectrom. Ion Processes **54**, 169 (1983).
19. J.H. Malmberg and T.M. O'Neil, Phys. Rev. Lett. **39**, 1333 (1977).
20. S. Ichimaru, I. Iyetomi, and S. Tanaka, Phys. Rep. **149**, 91 (1987).
21. E. Pollack and J. Hansen, Phys. Rev. A **8**, 3110 (1973); W.L. Slaterly, G.D. Doolen, and H.E. DeWitt, ibid. **21**, 2087 (1980); **26**, 2255 (1982); S. Ogata and S. Ichimaru, ibid. **36**, 5451 (1987); D.H.E. Dubin, ibid. **42**, 4972 (1990).
22. G. Birkl, S. Kassner, and H. Walther, Nature **357**, 310 (1992).
23. D.H.E. Dubin and T.M. O'Neil, Phys. Rev. Lett. **60**, 511 (1988).
24. A. Rahman and J.P. Schiffer, Phys. Rev. Lett. **57**, 1133 (1986).
25. H. Totsuji, in "Strongly Coupled Plasma Physics," edited by F.J. Rogers and H.E. Dewitt (Plenum, New York, 1987) p. 19.
26. D.H.E. Dubin, Phys. Rev. A **40**, 1140 (1989).
27. R.W. Hasse and V.V. Avilov, Phys. Rev. A **44**, 4506 (1991).
28. C. Kittel, "Introduction to Solid State Physics, Fourth Edition," (John Wiley, New York, 1971), Chap. 2.
29. D.H.E. Dubin, Phys. Rev. Lett. **66**, 2076 (1991).
30. T.J. Murphy, and C.M. Surko, Phys. Rev. A **46**, 5696 (1992).
31. G. Gabrielse, L. Haarsma and K. Abdullah, "Trapped positrons for antihydrogen and ion cooling", submitted for publication.
32. G. Gabrielse, X. Fei, L.A. Orozco, R.L. Tjoelker, J. Haas, H. Kalinowsky, T.A. Trainor, and W. Kells, Phys. Rev. Lett. **65**, 1317 (1990).
33. M.D. Tinkle, R.G. Greaves, C.M. Surko, R.L. Spencer, and G.W. Mason, Phys. Rev. Lett. **72**, 352 (1994).
34. R.G. Greaves, M.D. Tinkle, and C.M. Surko, submitted for publication.
35. D.J. Wineland and H.G. Dehmelt, J. Appl. Phys. **46**, 919 (1975).
36. Stephan Barlow, Ph. D. Thesis, Dept. of Physics, University of Colorado, 1984.
37. J. J. Bollinger, D. J. Heinzen, W. M. Itano, S. L. Gilbert, and D. J. Wineland, IEEE Trans. on Instrum. and Measurement **40**, 126 (1991).
38. W. M. Itano, J. C. Bergquist, J. J. Bollinger, J. M. Gilligan, D. J. Heinzen, F. L. Moore, M. G. Raizen, and D. J. Wineland, Phys. Rev. A **47**, 3554 (1993).
39. J.J. Bollinger, J.D. Prestage, W.M. Itano, and D.J. Wineland, Phys. Rev. Lett. **54**, 1000-1003 (1985).
40. D. J. Wineland, J. C. Bergquist, J. J. Bollinger, W. M. Itano, F. L. Moore, J. M. Gilligan, M. G. Raizen, D. J. Heinzen, C. S. Weimer, and C. H. Manney, in "Laser Manipulation of Atoms and Ions", ed. by E. Arimondo, W. D. Phillips, and F. Strumia (North-Holland, Amsterdam, 1992), pp. 553-567.
41. D. J. Wineland, J. C. Bergquist, J. J. Bollinger, W. M. Itano, D. J. Heinzen, S. L. Gilbert, C. H. Manney, and M. G. Raizen, IEEE Trans. on Ultrasonics, Ferroelectrics, and Frequency Control **37**, 515 (1990).
42. J. N. Tan, J. J. Bollinger, and D. J. Wineland, Proc. Conf. Prec. Electromagnetic Meas., Boulder, CO, June, 1994; to be published in special issue of IEEE Trans. Instrum. Meas.
43. T. M. O'Neil, Phys. Fluids **24**, 1477 (1981).

44. For a forthcoming review, see: "Proceedings of the Nobel Symposium on Trapped Charged Particles and Related Fundamental Physics, Lysekil, Sweden, August, '94", to be published in Physica Scripta.
45. D. J. Wineland, C. S. Weimer, and J. J. Bollinger, "Proc. of the Anti Hydrogen workshop, Munich, July 30-31, 1992", ed. by J. Eades, in Hyperfine Interactions 76, 115 (1993).
46. G. Gabrielse, S. L. Rolston, L. Haarsma, and W. Kells, Phys. Lett. A **129**, 38 (1988).
47. J.D. Prestage, J.J. Bollinger, W.M. Itano, and D.J. Wineland, Phys. Rev. Lett. **54**, 2387-2390 (1985).
48. J. J. Bollinger, D. J. Heinzen, W. M. Itano, S. L. Gilbert and D. J. Wineland, Phys. Rev. Lett. **63**, 1031 (1989).
49. D. J. Wineland, J. J. Bollinger, D. J. Heinzen, W. M. Itano, and M. G. Raizen, Phys. Rev. Lett. **67**, 1735 (1991).
50. R.G. Hulet, D.J. Wineland, J.C. Bergquist, and W.M. Itano, Phys. Rev. A **37**, 4544 (1988).
51. W. M. Itano, D. J. Heinzen, J. J. Bollinger, and D. J. Wineland, Phys. Rev. A **41**, 2295 (1990).
52. "Trapped Ions and Laser Cooling", ed. by D.J. Wineland, W.M. Itano, J.C. Bergquist and J.J. Bollinger, NBS Technical Note 1086 (1985); "Trapped Ions and Laser Cooling II", ed. by D. J. Wineland, W. M. Itano, J. C. Bergquist, and J. J. Bollinger, NIST Technical Note 1324, 1988; "Trapped Ions and Laser Cooling III," NIST Technical Note 1353, ed. by J. C. Bergquist, J. J. Bollinger, W. M. Itano, and D. J. Wineland (U. S. Government Printing Office, Washington, 1992).